AD-A104 507 BOSTON COLL CHESTNUT HILL MA DEPT OF PHYSICS F/G 20/8
PARTICLE TRAJECTORIES IN A MODEL ELECTRIC FIELD I,(U)
JUN 81 Y SHIMA, G KALMAN, P CARINI F19628-79-C-0031
UNCLASSIFIED SCIENTIFIC-1 AFGL-TR-81-0167 NL

1 OF 1
AD A
104507

END
DATE
FILMED
10-81
DTIC

LEVEL

12

BS

AFGL-TR-81-0167

AD A104507

PARTICLE TRAJECTORIES IN A
MODEL ELECTRIC FIELD I

Yaakov Shima
Gabor Kalman
Paul Carini

Boston College
Department of Physics
Chestnut Hill, Massachusetts 02167

Scientific Report No. 1

5 June 1981

Approved for public release; distribution unlimited

AIR FORCE GEOPHYSICS LABORATORY
AIR FORCE SYSTEMS COMMAND
UNITED STATES AIR FORCE
HANSCOM AFB, MASSACHUSETTS 01731

UNCLASSIFIED

SECURITY CLASSIFICATION OF THIS PAGE (When Data Entered)

REPORT DOCUMENTATION PAGE

READ INSTRUCTIONS BEFORE COMPLETING FORM

1. REPORT NUMBER: AFGL-TR-81-0167	2. GOVT ACCESSION NO.: AD-A104 507
3. RECIPIENT'S CATALOG NUMBER	
4. TITLE (and Subtitle): Particle Trajectories in a Model Electric Field I	5. TYPE OF REPORT & PERIOD COVERED: Scientific-[redacted]-1
	6. PERFORMING ORG. REPORT NUMBER
7. AUTHOR(s): Yaakov/Shima, Gabor/Kalman, Paul/Carini	8. CONTRACT OR GRANT NUMBER(s): F19628-79-C-0031
9. PERFORMING ORGANIZATION NAME AND ADDRESS: Boston College, Department of Physics, Chestnut Hill, MA 02167	10. PROGRAM ELEMENT, PROJECT, TASK AREA & WORK UNIT NUMBERS: 62101F, 76610605
11. CONTROLLING OFFICE NAME AND ADDRESS: Air Force Geophysics Laboratory, Hanscom AFB, Massachusetts 01731, Monitor/David A. Hardy Lt/PHG	12. REPORT DATE: 5 Jun[redacted]981
	13. NUMBER OF PAGES: 13
14. MONITORING AGENCY NAME & ADDRESS (if different from Controlling Office)	15. SECURITY CLASS. (of this report): UNCLASSIFIED
	15a. DECLASSIFICATION DOWNGRADING SCHEDULE

16. DISTRIBUTION STATEMENT (of this Report)

Approved for public release; distribution unlimited

17. DISTRIBUTION STATEMENT (of the abstract entered in Block 20, if different from Report)

18. SUPPLEMENTARY NOTES

19. KEY WORDS (Continue on reverse side if necessary and identify by block number)

Particle Trajectories
Surface Discharging

20. ABSTRACT (Continue on reverse side if necessary and identify by block number)

The work reported in this note was done for the purpose of determining the feasibility of neutralizing the potential difference that occurs on a spacecraft. It has been proposed that neutralization can be accomplished by emitting ions from the positively charged surface region of the spacecraft and by letting this current impact on the negatively charged surface region. In order to investigate the main features of the proposed scheme, we made some simplifying assumptions about the geometry of the problem. We

DD FORM 1 JAN 73 1473 EDITION OF 1 NOV 65 IS OBSOLETE

SECURITY CLASSIFICATION OF THIS PAGE (When Data Entered)

4:4609

approximated the geometry by two conducting infinite half planes and investigated the trajectories of a positive ion emitted at some point on the positively charged infinite half plane with given initial velocity and a given direction of emission.

A

I. INTRODUCTION

The work reported in this note was done for the purpose of determining the feasibility of neutralizing the potential difference that occurs on a spacecraft. It has been proposed that neutralization can be accomplished by emitting ions from the positively charged surface region of the spacecraft and by letting this current impact on the negatively charged surface region. In order to investigate the main features of the proposed scheme, we made some simplifying assumptions about the geometry of the problem. We approximated the geometry by two conducting infinite half planes and investigated the trajectories of a positive ion emmitted at some point on the positively charged infinite half plane with given initial velocity and a given direction of emission.

II. MATHEMATICAL STATEMENT OF THE PROBLEM

We consider the plane y=o and assume a cut on this plane along the z axis. Let there be a given potential difference V between the two half planes $x > o$ and $x < o$.

The equations of motion of a charged particle in the electric field produced in such a configuration are

$$m\frac{d^2x}{dt^2} = -\frac{eV}{\pi} \frac{y}{x^2+y^2}$$

$$m\frac{d^2y}{dt^2} = +\frac{eV}{\pi} \frac{x}{x^2+y^2} \tag{1}$$

$$m\frac{d^2z}{dt^2} = 0$$

The motion of the particle in the z direction is given trivially by

$$z = v_{zo}t + z_o$$

where v_{z_o} is the initial velocity and z_o is the initial position in the z direction. The x-y motion in the x-y plane is on which we focus. No analytic integral even of this simplified model equation could be found.

We can make use of the two (energy and angular momentum) integrals

$$\tfrac{1}{2}m\left(\left(\frac{d^2x}{dt}\right)^2 + \left(\frac{dy}{dt}\right)^2\right) - \frac{eV}{\pi}\ \mathrm{tg}^{-1}\frac{y}{x} = \tfrac{1}{2}m\ (v_{xo}^2 + v_{yo}^2)$$

$$y\frac{dx}{dt} - x\frac{dy}{dt} + \frac{eV}{m\pi}t = x_o v_{yo} \tag{2}$$

where the initial velocities of the particle are v_{x_o} and v_{y_o}, and the initial position is $x = x_o$, $y = o$.

In polar coordinates

$$x = r\cos\theta$$

$$y = r\sin\theta$$

the equations of motion become

$$(\ddot{r} - r\dot{\theta}^2)\cos\theta - (2\dot{r}\dot{\theta} + r\ddot{\theta})\sin\theta = -\frac{\beta}{r}\sin\theta$$

$$(2\dot{r}\dot{\theta} + r\ddot{\theta})\cos\theta + (\ddot{r} - r\dot{\theta}^2)\sin\theta = +\frac{\beta}{r}\cos\theta \tag{3}$$

with

$$\beta = \frac{eV}{m\pi} \tag{4}$$

These equations can be combined into

$$2\dot{r}\dot{\theta} + r\ddot{\theta} = \frac{\beta}{r} \tag{5}$$

and

$$\ddot{r} - r\dot{\theta}^2 = 0 \tag{6}$$

Eq. (5) can be simplified to

$$\frac{d}{dt}(r^2\dot{\theta}) = \beta \tag{7}$$

which provides the angular momemtum integral

$$r^2\,\dot{\theta} = r_o v_{yo} + \beta \quad 1 \tag{8}$$

Eq. (6) shows that $\ddot{r} > 0$ always, thus if $\dot{r}(0) \geq 0$, r itself also increases all the time.

The energy integral is obtained from (6) through multiplication by $\dot{r}$, and using (7):

$$\tfrac{1}{2}(\dot{r}^2 + r^2\,\dot{\theta}^2) - \beta\,\theta = \tfrac{1}{2}\,v_o^{\,2} \tag{9}$$

$$v_o^2 = v_{x_o}^2 + v_{y_o}^2 \quad ,$$

$$r_o = x_o$$

Eliminating $\dot{\theta}$ from (6) with the aid of (8), we obtain a second order differential equation for r:

$$\frac{d^2r}{dt^2} = \frac{(\beta t + r_o v_{yo})^2}{r^3} \tag{10}$$

which becomes

$$\frac{d^2f}{du^2} = \frac{u^2}{f^3} \tag{11}$$

after making the transformation

$$u = \beta t + r_o v_{yo}$$

$$f = \sqrt{\beta}\;\; r \tag{12}$$

A second order differential equation for the angle θ can also be obtained, although it is of limited interest only:

$$\left(\frac{d\theta}{du} - u\,\frac{d^2\theta}{du^2}\right)^2 = 4u\left(\frac{d\theta}{du}\right)^3 \left(2\left(\theta + \frac{\tfrac{1}{2}v_o^2}{\beta}\right) - u\,\frac{d\theta}{du}\right) \tag{13}$$

The differential equation of the trajectories can be obtained by eliminating t (or u). From (7) we have

$$r^2\dot{\theta} \quad \frac{d}{d\theta}(r^2\dot{\theta}) \quad = \quad \tfrac{1}{2}\frac{d}{d}\theta\,(r^4\dot{\theta}^2) \quad = \quad \beta r^2 \tag{14}$$

Eliminating $\dot{\theta}$ with the aid of (8), this results in

$$f^2 = \frac{d}{d\theta}\left(f^4 \frac{\theta + \frac{\frac{1}{2}v_o^2}{\beta}}{f^2 + (\frac{df}{d\theta})^2}\right) \tag{15}$$

III. NUMERICAL SOLUTIONS

The equations of motion (1) can be cast in a dimensionless form

$$\frac{d^2x}{dt^2} = -\frac{y}{x^2 + y^2}$$

$$\frac{d^2y}{dt^2} = +\frac{x}{x^2 + y^2}$$

with the initial conditions that at time t=o

$$x = 1$$

$$y = 0$$

$$v_x = v_{xo}$$

$$v_y = v_{yo}$$

where the initial velocities v_{xo} and v_{yo} are in units of $\sqrt{\beta}$, $\beta = \frac{eV}{m\pi}$.

We solved numerically this set of differential equations with the help of a subroutine DHPCG based on the Hamming's Modified Predictor Corrector Method. We assumed various initial conditions for v_{xo}, v_{yo}.

In the Table we give some results for cases where there is no initial velocity in the perpendicular direction, that is $v_{yo} = 0$, and the inital horizontal motion is towards the center. Also $v_{z_o} = 0$. x_* is the distance, from the center, of the point where the positive ion impacts on the negatively charged half plane. y_{max} is the maximum value of the y coordinate of the particle along its trajectory. Note that our results, up to $-v_{xo} \simeq 3.5$ are smooth in the sense that as $-v_{xo}$ increases, x_* decreases. At $-v_{xo} = 4$, and higher values, the results are not reliable. Whether the problem is in the numerical procedure is not clear at the present time.

Fig.-s 1, 2, and 3 portray families of particle trajectories with different initial conditions. In Fig. 1, the initial velocity is in the x-direction. It is clear that as v_{xo} increases, the impact distance, x_* is drastically reduced. Whether there is an optimum initial velocity, corresponding to a minimum impact distance, cannot be determined before the computational problem referred to above, is clarified. In Fig. 2, the initial velocity is in the y-direction. Here the impact distance <u>increases</u> with increasing velocity. In Fig. 3, the absolute value of the initial velocity is kept constant, while the direction of the emission is varied. There is a critical angle, θ_o, at which the impact distance is the same as for $v_o = 0$. For $\theta < \theta_o$ the impact distance is reduced, for $\theta > \theta_o$ it is increased. With the chosen $v_o = 0.1$, $\theta_o \simeq 83^o$. Figs. 4, 5, 6 give a more detailed picture of the dependence of the impact distance and of the maximum height of the trajectory on the parameters.

$-v_{x_0}$	x_*	time	y_{max}	time
0	750	320	50	120
0.2	390	160	25	60
1	55	23	3.7	8.8
2	25	7.9	0.9	3
2.5	10	3.9	0.6	1.2
3	2	1		
3.5	4.7	1.5	0.66	0.5
4	2000	390	26	140
4.5	2.2	0.7	0.14	0.45
5	5	1.2	0.21	0.47
5.5	5	1	0.15	0.5

CAPTIONS FOR FIGURES

FIG. 1 Trajectories for various initial velocities in the horizontal direction. The impact distance decreases with increasing velocity.

FIG. 2 Trajectories for various initial velocities in the vertical direction. The impact distance increases with increasing velocity.

FIG. 3 Trajectories for various initial emission angles. The impact distance increases with increasing angle.

FIG. 4 The impact distance (x_*) and the maximum height of the trajectary (y_m) as functions of the initial vertical velocity.

FIG. 5 The impact distance (x_*) and the maximum height of the trajectary (y_m) as functions of the initial horizontal velocity.

FIG. 6 The impact distance (x_*) and the maximum height of the trajectary (y_m) as functions of the angle of emission. Note that there is a critical angle θ_0, where $x_* (\theta_0, v_0) = x_* (v_0 = 0)$.

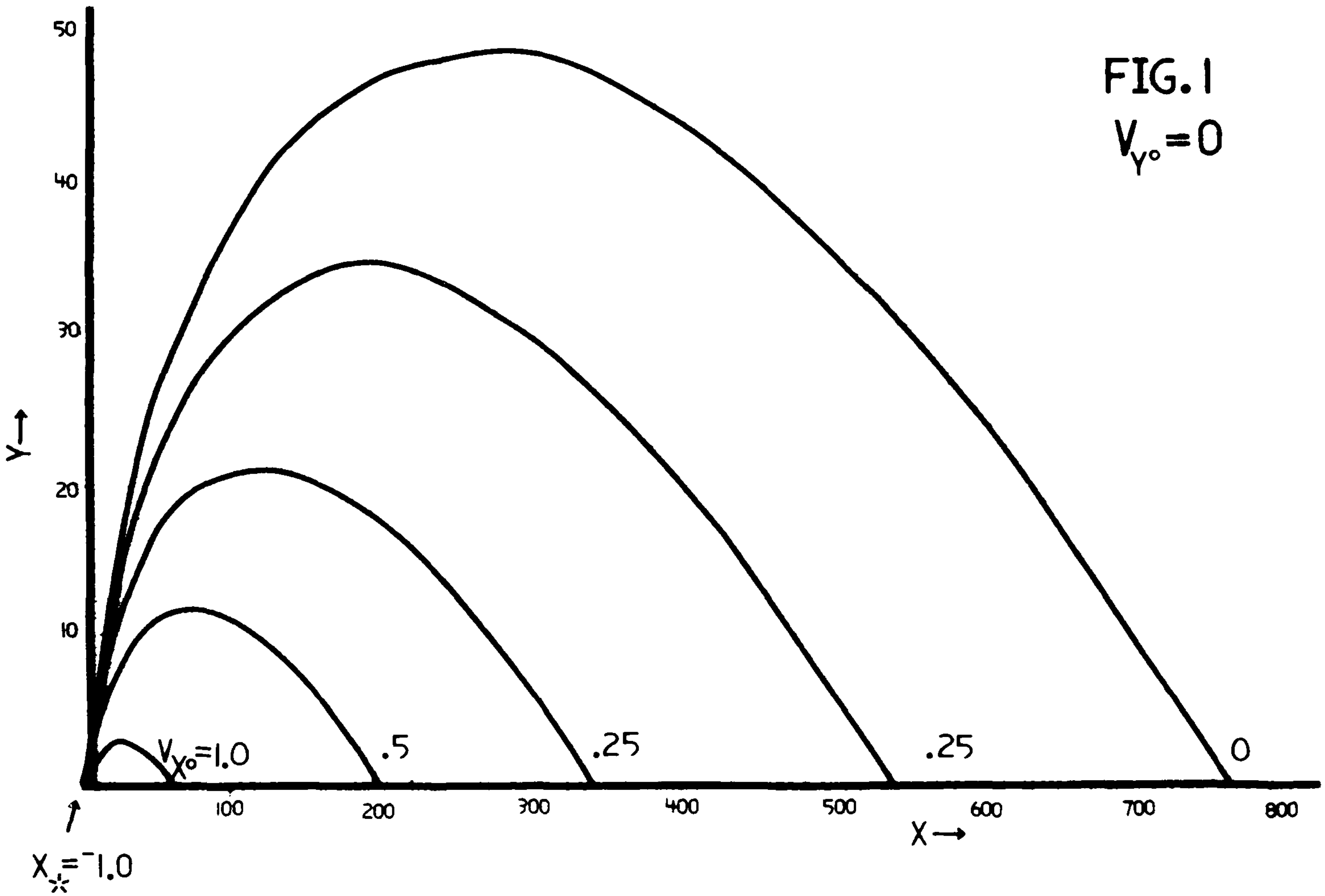

FIG. 1
$V_{Y°} = 0$

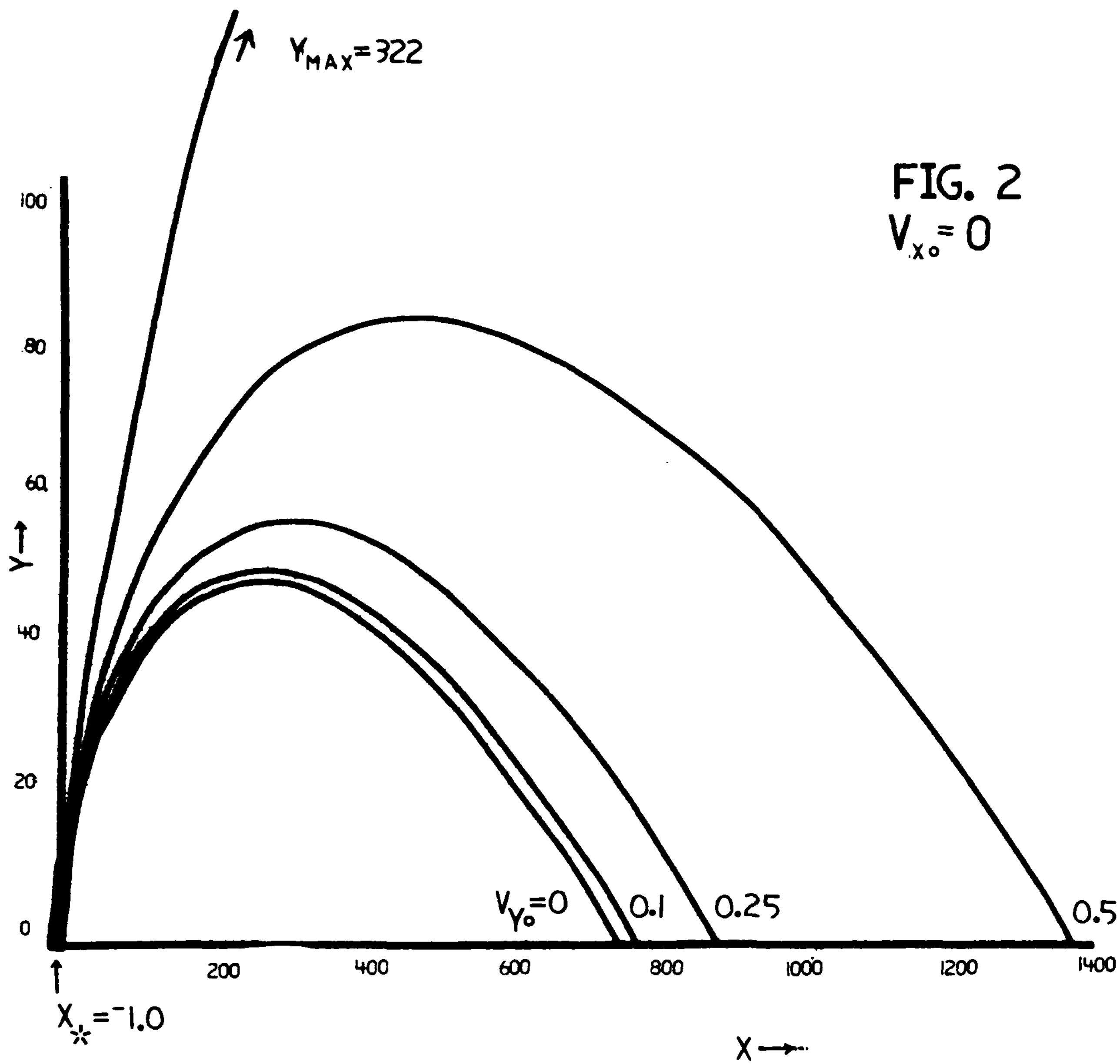
$Y_{MAX}=322$
100
80
60
40
20
0
$Y \longrightarrow$
200
400
600
800
1000
1200
1400
$X_{*}={}^{-}1.0$
$X \longrightarrow$
$V_{Y_0}=0$
0.1
0.25
0.5

FIG. 2
$V_{X_0}=0$

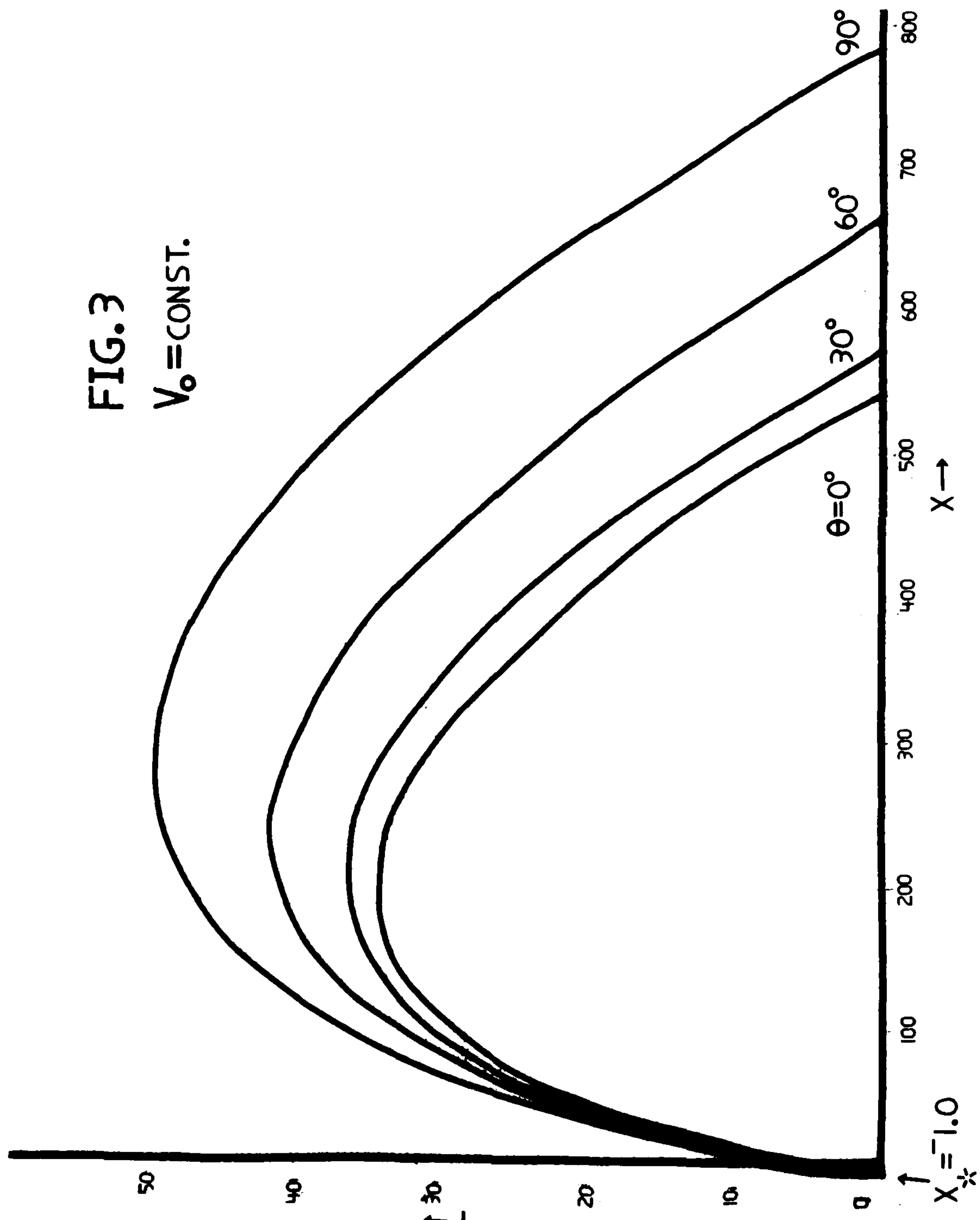

FIG. 3

V_o=CONST.

FIG. 4
$V_{x0} = 0$

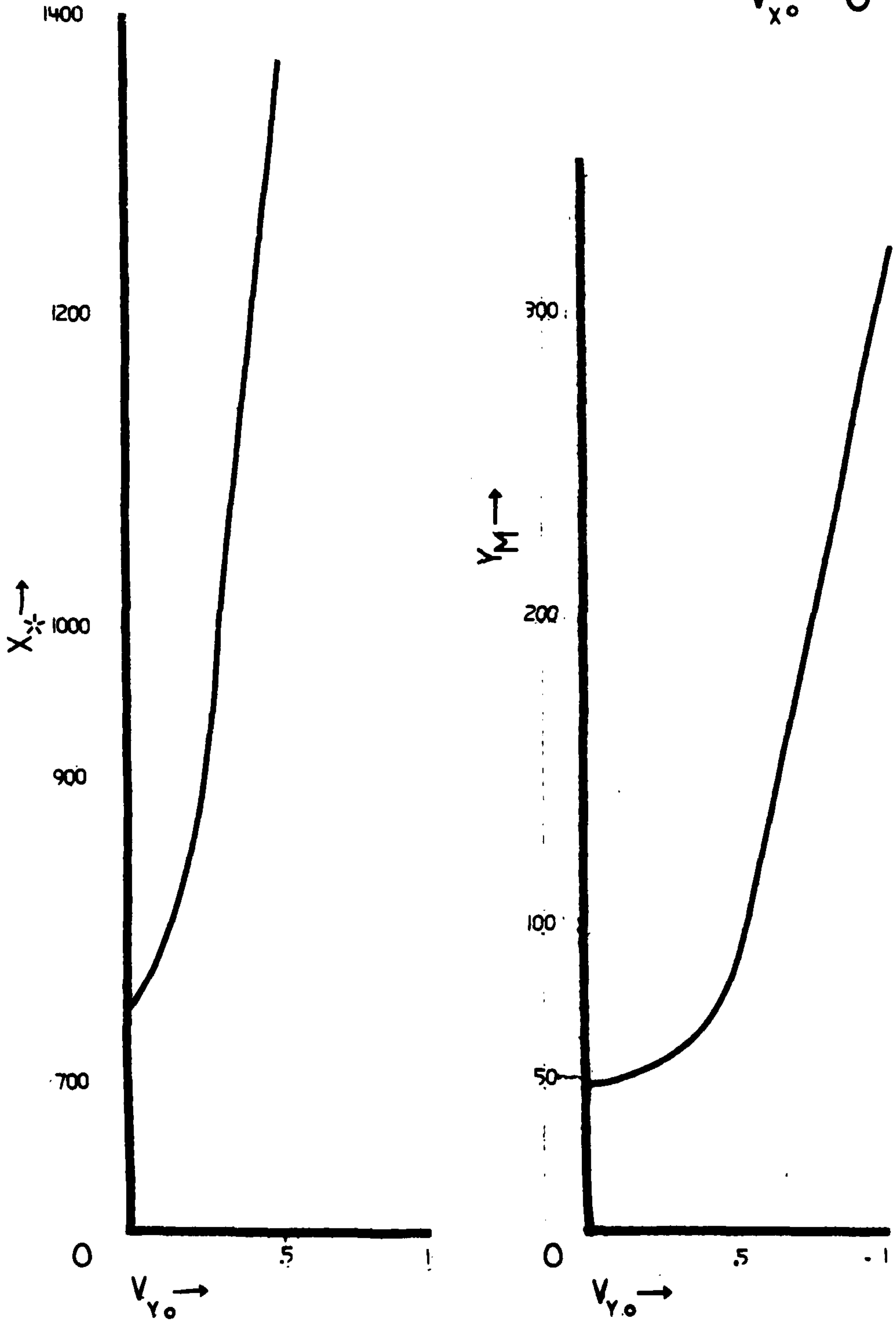

FIG. 5

$V_{Y0} = 0$

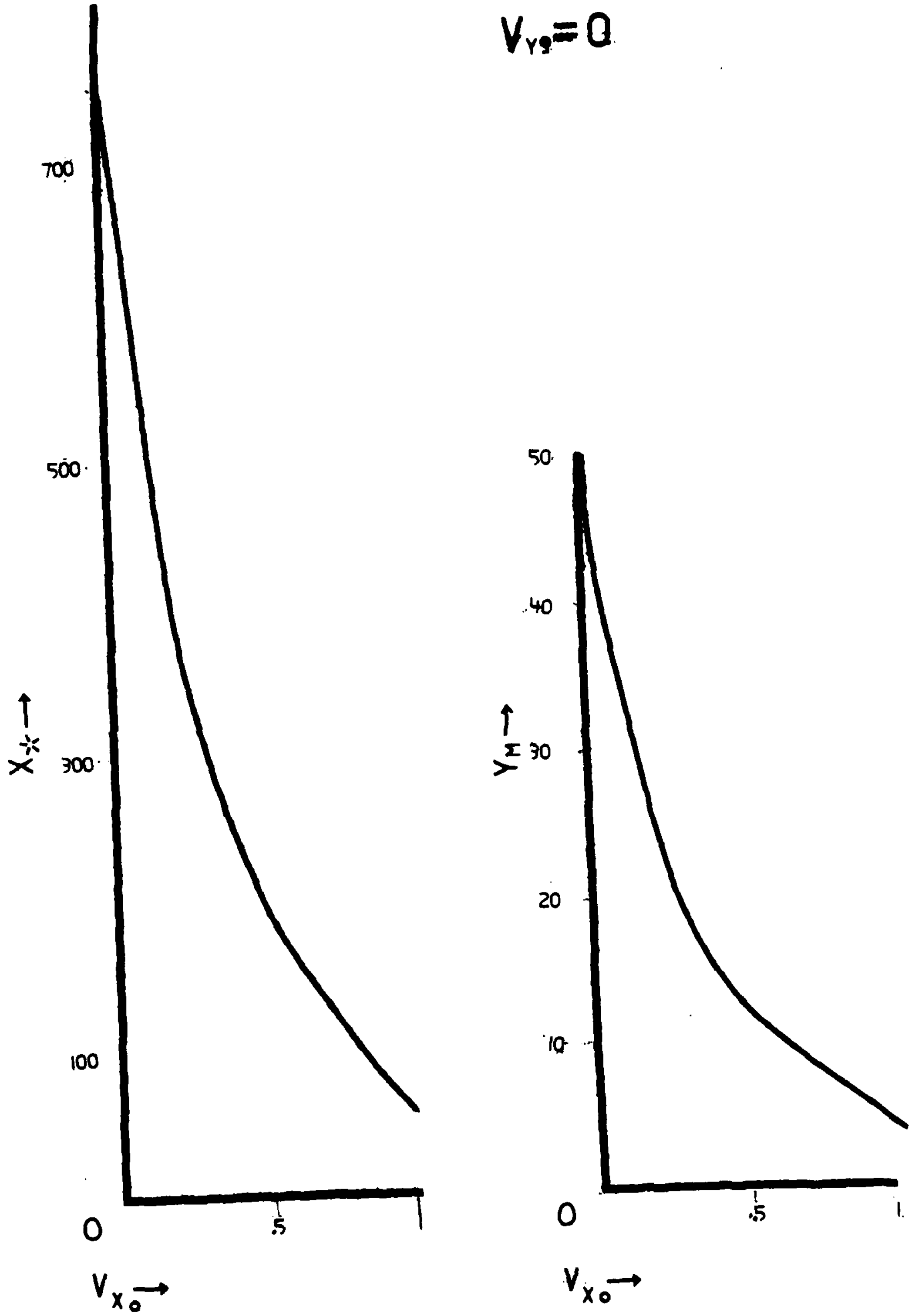

FIG.6

V_o=CONST.